

## Local modulation of the quantum-well quasicontinuum states using charged-carrier transfer induced by intersubband transitions

M. Bendayan\*

*Solid State Institute and Physics Department, Technion, Israel Institute of Technology, Haifa 32000, Israel*

R. Kapon

*Division of Applied Physics, The Fredi and Nadine Herrmann School of Applied Science, The Hebrew University of Jerusalem, Jerusalem 91904, Israel*

R. Beserman

*Solid State Institute and Physics Department, Technion, Israel Institute of Technology, Haifa 32000, Israel*

A. Sa'ar

*Division of Applied Physics, The Fredi and Nadine Herrmann School of Applied Science, The Hebrew University of Jerusalem, Jerusalem 91904, Israel*

R. Planel

*Laboratoire de Microstructures et Microelectronique, CNET, 196 Avenue Henri Ravera, Boîte Postale 107, 92225 Bagneux, France*

(Received 22 May 1997)

By generating a local electric field across an asymmetrical coupled quantum-well structure and using resonant Raman spectroscopy as a probe, we were able to resolve two classes of continuum electronic states of energies close to the barrier height. The first class is related to a continuum resonant state that is located near the edge of the barrier and is extended across the barrier region but not across the coupled quantum wells. The second class of continuum states is related to a quasibound resonant state that is localized above the quantum wells. Therefore, a local electric field across the coupled quantum wells modifies the energy spectrum of the localized resonant state while keeping the delocalized resonance unaffected. In our experiment the local electric field was generated by intersubband photoexcitation of carriers from one quantum well to the other. We observed a redshift of the quasibound resonant state due to the intersubband photoexcitation. [S0163-1829(97)02039-0]

The continuum electronic states above the barrier of a quantum-well (QW) structure play an important role in processes such as photoexcitation of bound carriers and in transport of photoexcited carriers across the QW structure. However, two different classes of continuum electronic states participate in these processes. The first class is related to quasibound resonant states for which a large fraction of the electronic envelope wave function is localized above the QW region. These states can be viewed as the analogs of the Fabry-Pérot resonances for which an integer number times half the De Broglie wavelength (of the envelope wave function) is equal to the well width. Because of the relatively large overlap between the envelope wave-functions of the continuum resonances and the QW bound states, it is expected that these resonances will play a major role in optical excitation of bound carriers to the continuum. The second class of continuum states is related to states that are not localized above the QW but rather extended along the barrier region, i.e., the probability to find a carrier above the barrier is much larger than the probability to find it above the QW. These states can be considered as resonances of the barrier region, however, since in most cases the barrier region is much larger than the QW, they are treated as a quasicontinuum. Although not frequently discussed in the literature, it is clear that these states should play an important role in coherent transport above the QW's.

In recent years there were several attempts to resolve these states and their physical behavior. Despite many efforts, routinely used experimental tools such as absorption spectroscopy and photoluminescence excitation spectroscopy, that can easily resolve bound states, have failed to reveal continuum resonances. We believe that the reason for that is the extremely fast relaxation processes (elastic and phonon assisted relaxation) that merge the absorption resonances into a quasicontinuum. To overcome this problem it has been proposed to increase the localization of the resonant states by using a variety of schemes such as Bragg confinement of the resonances<sup>1,2</sup> and by utilizing quarter wave electron stacks.<sup>3,4</sup> Using these methods one can get a larger degree of localization of the continuum resonances and observe intersubband optical transitions into these states.

In this report we provide experimental evidence for the existence of the two classes of continuum resonances discussed above and show that under the appropriate conditions one can resolve them. For that purpose, we generated a local electric field across the QW (but not along the barrier region) that modifies the energy spectrum of the quasilocalized resonances while leaving the delocalized continuum states unaffected. Such a local field can be generated, for example, in an asymmetrical coupled QW's (CQW) structure for which intersubband optical excitation induces charged carrier transfer

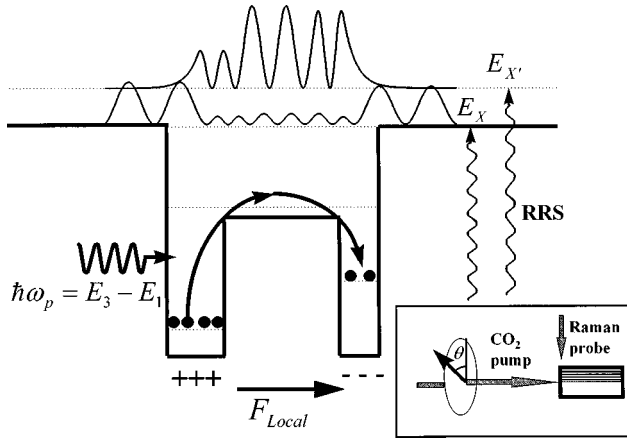


FIG. 1. Schematic of the coupled quantum-well structure used in our experiments. Shown are the energy levels and the envelope wave functions of the extended and the localized resonant continuum states. Also shown is the intersubband excitation process and the charge carrier transfer from the wide QW into the narrow QW that causes the formation of a local electric field across the CQW. The inset shows the experimental arrangement with the Raman probe beam and the polarized CO<sub>2</sub> laser beam.

from one QW to the other<sup>5</sup> thus leading to a formation of a local field across the CQW (see Fig. 1). For probing the influence of the local field on the continuum states we used resonant Raman scattering (RRS) spectroscopy. As shown by Zucker and co-workers and Wen and Chang,<sup>6–8</sup> this fully coherent process can reveal resonances in the continuum and is capable of detecting small energy shifts in these states.

The sample used in our experiments was grown by molecular beam epitaxy (MBE) on a GaAs semi-insulating substrate. It consists of 25 periods of asymmetric CQW's. Each period consists of a 5 nm wide GaAs QW, a 15 nm Al<sub>0.2</sub>Ga<sub>0.8</sub>As intermediate barrier, and a 7 nm wide GaAs QW. Each period is separated from the other by a 45 nm Al<sub>0.4</sub>Ga<sub>0.6</sub>As barrier and is modulation doped with Si to about  $4 \times 10^{11} \text{ cm}^{-2}$  at the center of the barrier. The whole structure is capped with a 15 nm GaAs top layer.

Figure 1 schematically shows the conduction band energy levels of a single period CQW. The energy spectrum was obtained by solving self-consistently the Ben Daniel-Duke and the Poisson equations for the conduction envelope states.<sup>9</sup> The lowest three bound subbands, that are involved in the intersubband optical excitation, have a confinement energy of 53, 80, and 176 meV, respectively. The structure was designed so that the lowest two subbands are localized in the wide and narrow QW's, respectively, while the third subband extends above both QW's. Ground-state carriers, that are localized in the wide QW, can resonantly be excited with a CO<sub>2</sub> laser (that operates at the 9.6 μm IR wavelength) into the third subband. In a steady state, a given fraction of the excited carriers (that is determined by the steady state solution of the rate equations to be discussed later on) are transferred into the first excited state of the narrow QW, giving rise to a local electric field across the CQW. The existence of intersubband transition from the ground to the third subband was verified by IR polarization resolved spectroscopy<sup>10</sup> using the intersubband selection rules.<sup>11</sup> The measured absorption coefficient of the transition was found

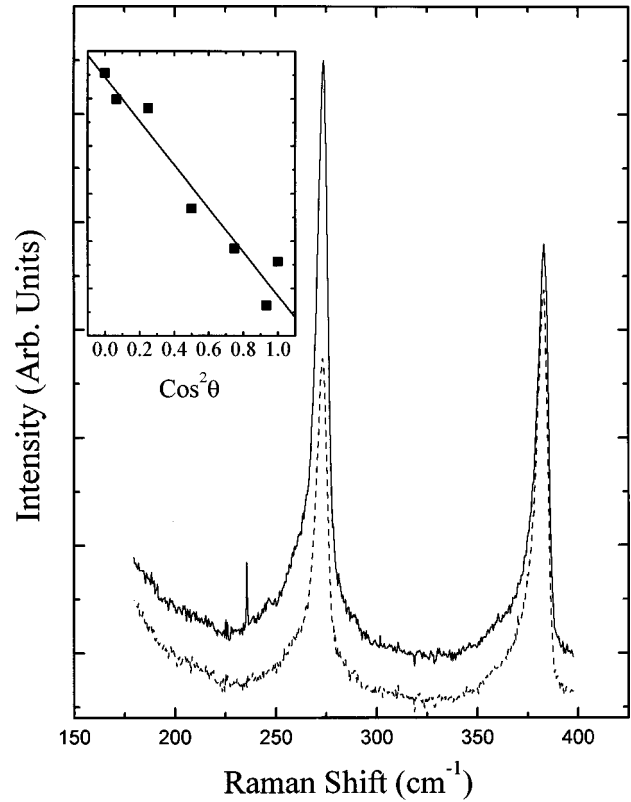


FIG. 2. Typical Raman scattering spectra taken at room temperature with the probe laser energy at 2.08 eV. Shown are spectra taken without (solid line) and with (dashed line) CO<sub>2</sub> laser illumination. The inset shows the change of the peak intensity of the GaAs mode as a function of  $\cos^2\theta$ , where  $\theta$  is the polarization angle of the CO<sub>2</sub> laser beam.

to be  $\alpha_{13}(\omega_p) \cong 100 \text{ cm}^{-1}$  per well, where  $\hbar\omega_p = \epsilon_3 - \epsilon_1 \cong 130 \text{ meV}$  is the peak absorption photon energy.

Next, the sample was cleaved into a stripe geometry and a CO<sub>2</sub> laser beam was focused into a 50 μm spot on the cleaved facet using a Ge lens. The power density of the CO<sub>2</sub> laser at the focal plane was about 150 kW/cm<sup>2</sup>. A quarter wavelength plate and a polarizer were used to rotate the incident polarization of the IR beam so that the intersubband selection rules could be verified.<sup>11</sup> Raman spectra were recorded in the backscattering configuration with a Dilor XY spectrometer. The beam of a R6G dye laser was focused on the sample through a microscope. The laser power was set to 10 mW and was kept constant during the experiment while the photon energy was tuned in the 2.03–2.15 eV range. The dye laser spot diameter is about 1.5 μm and was focused at a distance of about 10 μm from the cleaved edge (see inset of Fig. 1). Great care was taken in the alignment of the two laser beams to ensure that the dye laser probes the region that is excited by the CO<sub>2</sub> laser.

Figure 2 shows room temperature Raman spectra (with the probing dye laser energy set at 2.08 eV) taken with the CO<sub>2</sub> laser on (dashed line) and off (solid line). The spectra consist of GaAs-like and AlAs-like LO phonon modes of the Al<sub>0.4</sub>Ga<sub>0.6</sub>As layer (notice that the phonon modes of the GaAs and Al<sub>0.2</sub>Ga<sub>0.8</sub>As layers are too weak to be observed at that laser energy while at energies below 2.03 eV the lumi-

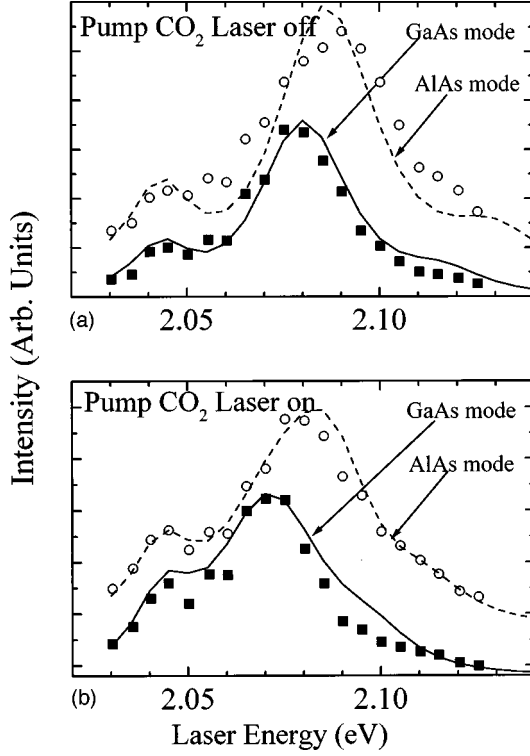


FIG. 3. Measured resonant Raman profiles (■ GaAs mode, ○ AlAs mode) and the profiles calculated using Eq. (1) (— GaAs mode, --- AlAs mode). Shown are the RRS (a) without CO<sub>2</sub> laser illumination and (b) with CO<sub>2</sub> laser illumination.

nescence background was too strong for observing Raman spectra). Similar spectra were obtained within the tuning range of the dye laser.

The effect of the CO<sub>2</sub> laser on the Raman spectrum is a significant reduction in the peak of the GaAs-like mode while keeping the peak of the AlAs-like mode unchanged. To ensure that the change in the peak intensity of the GaAs-like mode is related to the intersubband excitation, we measured the change in the peak intensity versus the polarization angle of the IR beam. The inset of Fig. 2 shows a fit of the experimental data to  $\cos^2\theta$  (where  $\theta=0$  means a polarization along the growth direction) that clearly obeys the intersubband selection rules. Furthermore, from the measurement of the ratio between the Stokes and the anti-Stokes lines we have verified that heating effects are negligible.

Next, by varying the dye laser photon energy in the 2.03–2.15 eV range, we measured the resonant Raman profile of the GaAs-like and the AlAs-like modes with the CO<sub>2</sub> laser on and off. These are shown in Fig. 3. For each RRS profile one can observe two resonant peaks that originate from quasicontinuum electronic states. Note that the location of the low-energy peak at about 2.045 eV is the same for both phonon modes and is not affected by the CO<sub>2</sub> laser excitation (for both phonon modes). On the other hand the irradiation by the CO<sub>2</sub> laser gives rise to a red shift in the high-energy peak of the GaAs and AlAs modes.

Let us describe now a model that can explain the origin of the above experimental results. Using the Raman scattering tensor<sup>12</sup> one can describe the resonant Raman profile as follows:<sup>7,8,13</sup>

$$I(\hbar_L) \propto \left| \frac{\langle 0 | \vec{p} \cdot \hat{\epsilon}_s | X' \rangle \langle X' | H_{ep} | X \rangle \langle X | \vec{p} \cdot \hat{\epsilon}_L | 0 \rangle}{(\hbar\omega_L - E_X + i\Gamma_1)(\hbar\omega_L - \hbar\omega_p - E_{X'} + i\Gamma_2)} + \frac{\langle 0 | \vec{p} \cdot \hat{\epsilon}_s | X \rangle \langle X | H_{ep} | X' \rangle \langle X' | \vec{p} \cdot \hat{\epsilon}_L | 0 \rangle}{(\hbar\omega_L - E_{X'} + i\Gamma_1)(\hbar\omega_L - \hbar\omega_p - E_X + i\Gamma_2)} \right|^2, \quad (1)$$

where  $\vec{p}$  is the dipole transition operator,  $H_{ep}$  is the electron phonon interaction Hamiltonian,  $\hat{\epsilon}_L$  and  $\hat{\epsilon}_s$  are polarization unit vectors of the incident and scattered light, respectively,  $X$  and  $X'$  are two electronic states with energies  $E_X$  and  $E_{X'}$ , respectively,  $\hbar\omega_p$  is the phonon energy, and  $\Gamma_1$  and  $\Gamma_2$  are the linewidths of the transitions. Hence, according to our model  $E_X$  represents the energy of the delocalized continuum state and therefore, should be identical for all four resonant Raman spectra, shown in Fig. 2. From the individual Raman spectra, shown in Fig. 2, we find the LO phonon energy,  $\hbar\omega_p$ , being equal to 34 meV for the GaAs-like mode and 47 meV for the AlAs-like mode. These values are in excellent agreement with previously published data.<sup>14,15</sup> Therefore, the only adjustable parameter in our model is the energy of the localized resonant state  $E_{X'}$ , that is redshifted under CO<sub>2</sub> laser illumination. This energy, however, must be the same for both the GaAs-like and the AlAs-like modes. The solid and the dashed lines in Fig. 3 show our fitting of the experimental data to the expression of Eq. (1) under the above constraints. As seen, a fairly good agreement is obtained, particularly if one takes into account the above constraints and the few numbers of free parameters. From the fitting we find  $E_X = 2.043$  eV,  $E_{X'} = 2.083$  eV with the CO<sub>2</sub> laser off and a redshift of 18 meV of the  $E_{X'}$  level under CO<sub>2</sub> laser intersubband optical excitation. The linewidth of the electronic transitions is found to be 15–20 meV for all transitions shown in Fig. 3.

We interpret the lower energy continuum state  $E_X$  as a delocalized electronic state that lies just above the Al<sub>0.4</sub>Ga<sub>0.6</sub>As barrier.<sup>7</sup> This level, being a true quasicontinuum state that is extended along the barrier, is almost unlocalized above the CQW and therefore, is not sensitive to the local electric field across the CQW. The second electronic state  $E_{X'}$  is interpreted as the higher energy quasi-bound resonant state that is localized above the CQW. Therefore, charge carrier transfer that induces a local electric field across the CQW causes a redshift of this level.

Let us now estimate the local electric field that is generated by the charged-carrier transfer induced by the pump CO<sub>2</sub> laser. For the estimate of the amount of charged carriers that are transferred into higher subbands by the optical excitation we used the following rate equations:

$$\frac{d\rho_3}{dt} = \frac{I_p}{\hbar\omega_{31}} \sigma_{13}(\omega_p)(\rho_1 - \rho_3) - \frac{\rho_3}{\tau_3},$$

$$\frac{d\rho_2}{dt} = \frac{\rho_3}{\tau_{32}} - \frac{\rho_2}{\tau_{21}},$$

$$\frac{d\rho_1}{dt} = -\frac{I_p}{\hbar\omega_{31}} \sigma_{13}(\omega_p)(\rho_1 - \rho_3) + \frac{\rho_2}{\tau_{21}} + \frac{\rho_3}{\tau_{31}}, \quad (2)$$

where  $\rho_j$  is the carrier density (per cm<sup>2</sup>) of the  $j$ th subband,  $I_p$  is the pump CO<sub>2</sub> laser power density,  $1/\tau_{ij}$  is the intersub-

band relaxation rate between the  $i$ th and the  $j$ th subbands,  $1/\tau_3 = 1/\tau_{31} + 1/\tau_{32}$  is the total relaxation rate of the third subband,  $\omega_p$  is the pump frequency,  $\sigma_{13}$  is the pump absorption cross section given by  $\sigma_{13}(\omega_p) = \alpha_{13}(\omega_p)L_1/\rho_1$ , and  $L_1$  is the width of the wide QW. Assuming that the total number of carriers is conserved, a steady state solution of the above equations can be derived and the density of carriers in the second and a third subbands can be found. Notice that, under our experimental conditions we have  $\rho_2, \rho_3 \ll \rho_1$ . Therefore, ignoring changes in the ground-state population we get  $\rho_3 \cong I_p \sigma_{13} \tau_3 \rho_1 / \hbar \omega_{13}$  and  $\rho_2 \cong \rho_3 (\tau_{21} / \tau_{32})$ . The relaxation times between the third and the lower two subbands are dominated by the fast LO phonon assisted relaxation and are taken to be of the order of  $\sim 1$  ps.<sup>16</sup> The much longer thermally assisted tunneling time through the thick  $\text{Al}_{0.2}\text{Ga}_{0.8}\text{As}$  intermediate barrier is a substantive parameter for our estimate. Recent works have assigned this process to either acoustic phonon assisted tunneling or impurities and defect assisted tunneling.<sup>17,18</sup> Nevertheless, since the time constants involved in these processes are of the same order (200–500 ps), we will use an average value of  $\tau_{21} \approx 350$  psec for our estimate. This yields,  $\rho_3 \cong 2 \times 10^8 \text{ cm}^{-2}$  and  $\rho_2 \cong 7 \times 10^{10} \text{ cm}^{-2}$ . Hence, most of the contribution to the local electric field comes from carriers in the second subband. A simple estimate of the local electric field yields  $F_{\text{local}} \cong (e/\epsilon_r)\rho_2 \cong 9.5 \text{ kV/cm}$ , and therefore,  $\Delta E_{X'} \cong eF_{\text{local}}L_T \cong 26 \text{ meV}$ , where  $L_T$  is the total width of the CQW over which the resonant state is localized. A more accurate estimate of the redshift can be obtained by solving self-consistently the rate equations and the Ben Daniel Duke-Poisson coupled equations. This yields  $\Delta E_{X'} \cong 13.5 \text{ meV}$  in a reasonable agreement with the measured redshift taking into account the uncertainty in the value of the tunneling

time,  $\tau_{21}$ . We would like to point out that similar calculations for the heavy hole subbands would give an energy separation between the localized and the unlocalized continuum resonances of the order of 4 meV and a much smaller energy shift under intersubband excitation. Such a small energy separation can not be resolved in our experiment since the homogeneous linewidth of the resonant electronic states is of the order of 15–20 meV. This is about 3 times the linewidth associated with bound electronic states and is attributed to the stronger coupling of the resonant states to the rest of the continuum via elastic scattering processes.

In conclusion, using RRS as a probe we were able to resolve the effect of a local electric field, that is generated by intersubband optical excitation, on the resonant continuum electronic states above the barrier of a CQW structure. Two classes of resonant states have been observed. The first is located near the bottom of the barrier and is extended along the barrier region but not above the CQW. Therefore, this continuum state is not sensitive to the local electric field that is generated inside the CQW. The second class of continuum states is related to a quasibound resonant state that is localized above the CQW at a higher energy (relative to the delocalized resonant state). This state exhibits a redshift under a local electric field that is generated by charged carrier transfer from the wide QW into the narrow QW under intersubband optical excitation. Self-consistent calculations that takes into account charge-carrier transfer due to intersubband excitation provide a good estimate to the observed redshift of the localized resonant state. Both states have been found to be conduction resonances of the continuum.

This work has been partially supported by a joint grant of the Commission of European Communities and the Israeli Ministry of Science (EC No. CII\*-CT93-0072).

\*Present address: Rafael, POB 2250(88), Haifa 31021, Israel. Electronic address: michab@rafael.co.il

<sup>1</sup>M. Zahler, I. Brener, G. Lenz, J. Salzman, E. Cohen, and L. Pfeiffer, *Appl. Phys. Lett.* **61**, 949 (1992).

<sup>2</sup>G. N. Henderson, L. C. West, T. K. Gaylor, C. W. Roberts, E. N. Glytsis, and M. T. Asom, *Appl. Phys. Lett.* **62**, 1432 (1993).

<sup>3</sup>C. Sirtori, F. Capasso, J. Faist, D. L. Sivco, S. N. G. Chu, and A. Y. Cho, *Appl. Phys. Lett.* **61**, 898 (1992).

<sup>4</sup>C. Sirtori, J. Faist, F. Capasso, D. L. Sivco, and A. Y. Cho, *Appl. Phys. Lett.* **62**, 1931 (1993).

<sup>5</sup>H. Akiyama, H. Sugawara, Y. Kadoya, A. Lorke, S. Tsujuno, and H. Sakaki, *Appl. Phys. Lett.* **65**, 424 (1994).

<sup>6</sup>J. E. Zucker, A. Pinczuk, D. S. Chemla, A. Gossard, and W. Wiegmann, *Phys. Rev. B* **29**, 7065 (1984).

<sup>7</sup>J. E. Zucker, A. Pinczuk, and D. S. Chemla, *Phys. Rev. B* **38**, 4287 (1988).

<sup>8</sup>G. Wen and Y. C. Chang, *Phys. Rev. B* **45**, 13 562 (1992).

<sup>9</sup>G. Bastard, *Wave Mechanics Applied to Semiconductor Hetero-*

*structures* (Halsted, 1988).

<sup>10</sup>See, for example, *Quantum Well Intersubband Transition Physics and Devices*, NATO Advanced Study Institute Series E: Applied Physics, Vol. 270 (Kluwer, Dordrecht, 1994), and references therein.

<sup>11</sup>A. Sa'ar, *J. Appl. Phys.* **74**, 5263 (1993).

<sup>12</sup>M. Cardonna, in *Light Scattering in Solids II*, edited by M. Cardonna and G. Guntherodt (1982), Chap. 2.

<sup>13</sup>J. E. Zucker, A. Pinczuk, D. S. Chemla, A. Gossard, and W. Wiegmann, *Phys. Rev. Lett.* **51**, 1293 (1983).

<sup>14</sup>L. Pavesi and M. Guzzi, *J. Appl. Phys.* **75**, 4779 (1994).

<sup>15</sup>S. Adashi, *J. Appl. Phys.* **58**, R1 (1985).

<sup>16</sup>J. Wang, J. P. Leburton, Z. Moussa, F. H. Julien, and A. Sa'ar, *J. Appl. Phys.* **80**, 1970 (1997).

<sup>17</sup>N. Sawaki, R. A. Hopfel, E. Gornik, and H. Kano, *Appl. Phys. Lett.* **55**, 1996 (1989).

<sup>18</sup>Ph. Roussignol, A. Vinattieri, L. Carraresi, M. Colocci, and A. Fasolino, *Phys. Rev. B* **44**, 8873 (1991).